

# Geometric phase gates in dissipative quantum dynamics

Kai Müller, Kimmo Luoma,\* and Walter T. Strunz

*Institut für Theoretische Physik, Technische Universität Dresden, D-01062, Dresden, Germany*

(Dated: June 6, 2022)

Trapped ions are among the most promising candidates for performing quantum information processing tasks. Recently, it was demonstrated how the properties of geometric phases can be used to implement an entangling two qubit phase gate with significantly reduced operation time while having a built-in resistance against certain types of errors (Palmero et. al., Phys. Rev. A **95**, 022328 (2017)). In this article, we investigate the influence of both quantum and thermal fluctuations on the geometric phase in the Markov regime. We show that additional environmentally induced phases as well as a loss of coherence result from the non-unitary evolution, even at zero temperature. We connect these effects to the associated dynamical and geometrical phases. This suggests a strategy to compensate the detrimental environmental influences and restore some of the properties of the ideal implementation. Our main result is a strategy for zero temperature to construct forces for the geometric phase gate which compensate the dissipative effects and leave the produced phase as well as the final motional state identical to the isolated case. We show that the same strategy helps also at finite temperatures. Furthermore, we examine the effects of dissipation on the fidelity and the robustness of a two qubit phase gate against certain error types.

## I. INTRODUCTION

During the last decades there has been an increasing effort to develop reliable, large scale quantum information processors. Since such a device could utilize quantum properties like superpositions and entanglement, its computing power could potentially surpass every conceivable classical device for certain problems [1, 2] with potential applications in various fields of science and technology. At the moment there are several physical realizations developed in parallel, each with their own benefits and drawbacks. One of the most advanced platforms for quantum information processing is based on trapped ions [3], where many elementary operations have already been experimentally demonstrated with high precision [4–6]. Up to date there are, however, still various difficulties to overcome [7]. One of the most severe issues is dissipation and decoherence resulting from the interaction of the quantum system with the environment leading to detrimental effects on the quantum resources and to quantum gate errors. Although there exist quantum error correction schemes that can compensate small errors of the quantum gates these only allow error rates of roughly 1% and come at the cost of a high computational overhead [8]. This means that in order to construct an efficient quantum information processor it is necessary to reduce the error rates of the individual quantum gates as much as possible. It is therefore important to have a good understanding of the environmental effects and how to compensate for them.

In this work we want to specifically focus on two-qubit phase gates, which perform the following operation

$$\begin{aligned} |00\rangle &\rightarrow |00\rangle, & |11\rangle &\rightarrow |11\rangle, \\ |01\rangle &\rightarrow e^{i\Phi}|01\rangle, & |10\rangle &\rightarrow e^{i\Phi}|10\rangle. \end{aligned} \quad (1)$$

Two-qubit phase gates are important since they can be used to convert the separable state  $1/2(|11\rangle + |10\rangle + |01\rangle + |00\rangle)$  into a maximally entangled state  $1/2(|11\rangle + i|10\rangle + i|01\rangle + |00\rangle)$ . First experimental implementations were realized over a decade ago [9, 10], based on theoretical proposals in [11–13]. However due to recent efforts in theory [14–17] and experimental techniques [18] the operation times and error rates have significantly reduced. These realizations leverage the idea of geometric phases first introduced by Berry [19, 20] where the cyclic evolution of a quantum state results in the acquisition of a phase. The aim of this article is to investigate the effects of quantum and thermal fluctuations on the geometric phase gate given by Eq. (1). We show how to extend the ideal (fluctuation free) implementation of the gate given in [14] in order to compensate the detrimental environmental effects.

The outline of the remainder of the article is the following. In Sec. II we first review the ideal isolated case, introduce our notation and then present our open system model in the context of a single trapped ion. In Sec. III we then show how dissipation leads to additional phases and in which way they can be connected to the conventional geometrical and dynamical phases. Furthermore we show which conditions the experimental protocol must satisfy in order to implement a phase gate and how the sensitivity of the gate against small experimental errors is altered compared to the case where the system is perfectly isolated from its environment. In IV we then apply our results to the two-qubit phase gate protocol proposed in [14] and examine the impact on the fidelity. In Sec. V we use the results of the previous sections to draw conclusions for the finite temperature case. We close the main part of the article with a summary and an outlook. Lastly, some of the analytic computations are presented in the Appendix.

\* kimmo.luoma@tu-dresden.de

## II. MODEL

In this section we will first introduce a model for an isolated phase gate. Then we expand the model to account for detrimental environmental effects.

### A. Isolated system

We consider the ion trap as a quantum harmonic oscillator with mass  $m$  and frequency  $\omega$  which is driven by an external force leading to the Hamiltonian

$$H_{\text{isol}}(t) = \hbar\omega a^\dagger a + V(t). \quad (2)$$

Here  $a$  ( $a^\dagger$ ) is the annihilation (creation) operator for the vibrational mode satisfying bosonic commutation relations  $[a, a^\dagger] = 1$ . The potential  $V(t)$  arises from the externally applied force  $F(t)$ . Since we want to implement the operation described in Eq. (1) we need to introduce state-dependent forces  $F_1$  and  $F_0$  that depend on an internal (e.g. spin-) state of the ion in order to distinguish these states. An ion in the internal state  $|1\rangle$  will only experience  $F_1$  and vice versa. In the following we will use the notation  $F_j$  with  $j = 0, 1$  labeling the internal state of the ion. Furthermore, the external forces  $F_j(t)$  are assumed to be homogeneous over the extent of the motional state. This can be assumed, for example, for forces realized by lasers if the wavelength of the laser is much greater than the amplitude of oscillation. Under these circumstances the Hamiltonian can be written in the following form

$$H(t) = \hbar\omega(a^\dagger a) + |0\rangle\langle 0| \otimes V_0(t) + |1\rangle\langle 1| \otimes V_1(t), \quad (3)$$

$$V_j(t) = F_j(t)x = f_j(t)(a + a^\dagger), \quad (4)$$

with  $f_j(t) = \frac{\hbar}{2m\omega}F_j(t)$ .

Before we determine the evolution of a quantum state in this model we will simplify the equations more by switching to an interaction picture with respect to  $\hbar\omega a^\dagger a$  leading to a simpler Hamiltonian

$$\tilde{H}(t) = |0\rangle\langle 0| \otimes \tilde{V}_0(t) + |1\rangle\langle 1| \otimes \tilde{V}_1(t), \quad (5)$$

$$\tilde{V}_j(t) = \tilde{f}_j^*(t)a + \tilde{f}_j(t)a^\dagger,$$

where  $\tilde{f}_j = e^{i\omega t}f_j$ . The equation of motion in the interaction picture for a quantum state represented by the density operator  $\rho$  is the von-Neumann equation

$$\dot{\rho} = -i\frac{1}{\hbar}[\tilde{H}(t), \rho]. \quad (6)$$

This equation can be solved by inserting an ansatz  $\rho = |\Psi_t\rangle\langle\Psi_t|$ , where

$$|\Psi_t\rangle = \sum_{j=0}^1 a_j e^{i\varphi_j(t)} |j, z_j(t)\rangle, \quad (7)$$

where  $j$  represents the internal state and  $|z_j(t)\rangle = e^{-|z_j(t)|^2/2} \sum_{n=0}^{\infty} ((z_j(t))^n / \sqrt{n!}) |n\rangle$  is a coherent state for the motional degree of freedom of the ion when the internal state is  $|j\rangle$ , ( $j = 0, 1$ ) and  $a_j$  is a constant determined from the initial conditions. Inserting this ansatz into Eq. (6) leads to the following equation for the coherent state label  $z_j(t)$

$$\dot{z}_j = \frac{1}{i\hbar} \tilde{f}_j(t). \quad (8)$$

In the context of implementing a phase gate, we want  $f_j(t)$  to be part of some protocol which is switched on at a certain time and is completed some time  $T$  later. Therefore  $f_j$  shall only be non-zero in the interval  $[0, T]$  and it shall be such that the motional state undergoes a cyclic evolution  $z_j(0) = z_j(T)$  whereas the internal degrees of freedom acquire a phase according to Eqs. (1). It is known that such a cyclic quantum evolution leads to the acquisition of a phase  $\varphi_j = \varphi_{g,j} + \varphi_{d,j}$ , where the dynamical and geometrical phases satisfy  $\dot{\varphi}_{d,j} = -(1/\hbar)\langle j, z_j(t) | H(t) | j, z_j(t) \rangle$  and  $\dot{\varphi}_{g,j} = i\langle j, z_j(t) | \partial_t | j, z_j(t) \rangle$ , respectively. The total phase acquired is equal to twice the area enclosed by the trajectory  $z_j(t)$  in the interaction picture (see Eq. (23)) [10, 14]. In the following we will expand this model to include quantum and thermal fluctuations.

### B. Open system

Effects of the ion coupling to some external environment are modeled phenomenologically by a Gorini-Kossakowski-Sudarshan-Lindblad (GKSL) master equation [21, 22] of the following form

$$\begin{aligned} \dot{\rho} = & -i\frac{1}{\hbar}[\tilde{H}(t), \rho] + \gamma(\bar{n} + 1)(2a\rho a^\dagger - a^\dagger a\rho - \rho a^\dagger a) \\ & + \gamma\bar{n}(2a^\dagger \rho a - a a^\dagger \rho - \rho a a^\dagger), \end{aligned} \quad (9)$$

in the interaction picture. The model (9) describes dissipation and thermal excitation of the motional state of the ion with rates  $\gamma(\bar{n} + 1)$  and  $\gamma\bar{n}$ , respectively.  $\bar{n}$  models the average occupation number of the bosonic heat bath modes at a relevant system frequency at finite temperature. At zero temperature,  $\bar{n} = 0$  and only quantum fluctuations and damping with rate  $\gamma$  are present.

Motional coherence times  $(\gamma\bar{n})^{-1}$  for the trapped ion systems are of the order of 1 - 100 milliseconds [7, 23]. Typical frequency for the harmonic motion of the ion around the minimum of the trap is in the MHz range, whereas operation times for the two qubit phase gate investigated later in the article is in the  $\mu\text{s}$  range [14].

As shown in [24, 25], finite temperature effects can be incorporated in the zero temperature model by adding a fluctuating force  $\sqrt{2\gamma\bar{n}\hbar}\chi(t)$  to the Hamiltonian. Here  $\chi(t)$  is a Gaussian white noise process with  $\langle\chi(t)\rangle = \langle\chi(t)\chi(t')\rangle = 0$  and  $\langle\chi(t)\chi^*(t')\rangle = \delta(t - t')$ . Thus the

Hamiltonian reads

$$\widetilde{H}_\chi(t) = |0\rangle\langle 0| \otimes \widetilde{V}_{0,\chi}(t) + |1\rangle\langle 1| \otimes \widetilde{V}_{1,\chi}(t), \quad (10)$$

$$\begin{aligned} \widetilde{V}_j(t) &= (\widetilde{f}_j^*(t) + \sqrt{2\gamma\bar{n}}\hbar\chi^*(t))a \\ &+ (\widetilde{f}_j(t) + \sqrt{2\gamma\bar{n}}\hbar\chi(t))a^\dagger. \end{aligned} \quad (11)$$

Note that the noise does not depend on the internal state  $j$ . The finite temperature model (9) is thus equivalent to an ensemble of zero temperature models with stochastic Hamiltonian

$$\dot{\rho}_\chi = -i\frac{1}{\hbar}[\widetilde{H}_\chi(t), \rho_\chi] + \gamma(2a\rho_\chi a^\dagger - a^\dagger a\rho_\chi - \rho_\chi a^\dagger a). \quad (12)$$

The evolution of the density operator can be recovered by taking an average over  $\chi(t)$

$$\rho(t) = \langle \rho_\chi(t) \rangle, \quad (13)$$

and the average state  $\rho(t)$  satisfies Eq. (9).

Remarkably, Eq. (12) can still be solved by a coherent state ansatz, such as Eq. (7), although it contains the effects of thermal and quantum fluctuations. Inserting the ansatz from Eq. (7) for a particle in the internal state  $|j\rangle$  into Eq. (9) leads to the following equation for the coherent state label  $z_j(t)$

$$\dot{z}_j + \gamma z_j = \frac{1}{i\hbar} \left( \widetilde{f}_j(t) + \sqrt{2\gamma\bar{n}}\hbar\chi(t) \right). \quad (14)$$

For current ion-traps the motional coherence time  $1/(\gamma\bar{n})$  is much longer than the operation time [7, 23] so that the motion of the ion is dominated by the deterministic force.

In the following sections we will first investigate the zero temperature case for an arbitrary force. In section V we can apply these results to a noisy force and average over the noise.

### III. CONSEQUENCES OF QUANTUM FLUCTUATIONS

In this section we investigate the consequences of coupling the trapped ion to a zero temperature bath. The effect of thermal fluctuations will be considered in Sec. V.

#### A. Consequences for the phase

In the following we want to investigate how the Lindblad terms in the time evolution equation affect the phase. We therefore consider a model which is in principle identical to (9) at zero temperature but slightly more general. The result can then be applied to the phase gate model.

The Hamiltonian shall be of the form

$$H(t) = |0\rangle\langle 0| \otimes H_0(t) + |1\rangle\langle 1| \otimes H_1(t),$$

where  $|0\rangle$ ,  $|1\rangle$  represent the internal states of the ion and  $H_0(t)$  and  $H_1(t)$  act on the motional degree of freedom. We assume that the dissipation and decoherence is well described by a general GKSL master equation and thus arrive at the following model

$$\dot{\rho} = \frac{-i}{\hbar} [H(t), \rho] + \mathcal{L}[\rho], \quad (15)$$

$$\mathcal{L}[\rho] = \sum_{l=1}^N L_l \rho L_l^\dagger - \frac{1}{2} \left( L_l^\dagger L_l \rho + \rho L_l^\dagger L_l \right).$$

Furthermore we assume that this model has a pure state solution  $|\Phi_t\rangle\langle\Phi_t|$ , where  $|\Phi_t\rangle = \sum_j |j\rangle \Psi_j(t)$  and the internal state  $j$  remains unchanged during the evolution. Although these are very limiting assumptions we will see that the results can nevertheless be applied to the phase gate scenario mentioned before.

Under these assumptions, we can repeat the argument proposed in [20] for a cyclic quantum evolution governed by a time-dependent Schrödinger equation to determine the relative phase that arises if the initial state is in a superposition of internal states. In our case, however, the cyclic quantum evolution of a pure state is modified by a damping term. The details of the computation can be found in the appendix A. We then get a new complex valued term  $\xi$  in addition to the dynamical and geometrical phase

$$\varphi = \varphi_g + \varphi_d + \xi, \quad (16)$$

$$\xi = \varphi_L + i\eta, \quad (17)$$

where the individual terms are defined as follows:

$$\begin{aligned} \dot{\varphi}_g &= i(\langle \Psi_0 | \partial_t | \Psi_0 \rangle - \langle \Psi_1 | \partial_t | \Psi_1 \rangle), \\ \dot{\varphi}_d &= -\frac{1}{\hbar} (\langle H_0(t) \rangle - \langle H_1(t) \rangle), \\ \dot{\xi} &= -i \sum_{l=1}^N \langle \Psi_0 | L_l | \Psi_0 \rangle \langle \Psi_1 | L_l^\dagger | \Psi_1 \rangle \\ &\quad - \frac{1}{2} \left( \langle \Psi_0 | L_l^\dagger L_l | \Psi_0 \rangle + \langle \Psi_1 | L_l^\dagger L_l | \Psi_1 \rangle \right). \end{aligned} \quad (18)$$

The first two terms are identical to the unitary case mentioned before and also found in [20]. Therefore, they correspond to dynamical and geometrical phases which arise during a cyclic evolution of a quantum system. Since we have constructed relative phases they are expressed as the difference between the dynamical/geometrical phases of particles in the internal states 0 and 1. The last sum cannot be expressed in such a way and contains dissipative effects. In general it leads to real terms in the exponent which result in a loss of coherence. We can apply this equation to the damped harmonic oscillator if we set  $L = \sqrt{\gamma}a$  and  $|\Psi_j\rangle = |j, z_j\rangle$ . Furthermore we can identify  $H_j(t)$ , which corresponds to the Hamiltonian seen by a particle in the internal state  $|j\rangle$  as  $\hbar\omega a^\dagger a + V_j(t)$  (see Eq. (3)). This means we can calculate the dynamical phase for a particle in the internal state  $j$  with  $|j, z_j\rangle$  in

the interaction picture by using Eqs. (14) and (5) as

$$\begin{aligned}
\varphi_{d,j} &= -\frac{1}{\hbar} \langle H_j(t) \rangle \\
&= \frac{-1}{\hbar} \int_0^T \langle j, z_j(t) | e^{-i\omega t a^\dagger a} H(t) e^{i\omega t a^\dagger a} | j, z_j(t) \rangle dt \\
&= \frac{-1}{\hbar} \int_0^T \langle j, z_j(t) | \hbar \omega a^\dagger a + \tilde{V}_j(t) | j, z_j(t) \rangle dt \\
&= \int_0^T 2 \operatorname{Im}(\dot{z}_j(t) z_j^*(t)) - \omega |z_j(t)|^2 dt. \tag{19}
\end{aligned}$$

For the geometric phase we arrive at

$$\begin{aligned}
\varphi_{g,j} &= i \left( \langle z_j(t) | e^{-i\omega t a^\dagger a} \partial_t e^{i\omega t a^\dagger a} | z_j(t) \rangle \right) \\
&= \int_0^T -\operatorname{Im}(\dot{z}_j(t) z_j^*(t)) + \omega |z_j(t)|^2 dt, \tag{20}
\end{aligned}$$

$$\tag{21}$$

again with  $|j, z_j\rangle$  in the interaction picture. As we can see the dynamical and geometrical phase are remarkably similar for the harmonic oscillator. Furthermore we can combine these two phases for the total phase in the isolated ( $\gamma = 0$ ) case  $\varphi_{\text{isol}}$ :

$$\begin{aligned}
\varphi_{\text{isol}} &= (\varphi_{d,0} - \varphi_{d,1}) + (\varphi_{g,0} - \varphi_{g,1}) \\
&= \int_0^T \operatorname{Im}((\dot{z}_0(t) z_0^*(t)) - \dot{z}_1(t) z_1^*(t)) dt. \tag{22}
\end{aligned}$$

For a cyclic evolution this reduces to the known result [10, 14]

$$\varphi_{\text{isol}} = 2(A_0 - A_1), \tag{23}$$

where  $A_j$  is the area enclosed by the cyclic evolution of  $z_j$ . This is shown in Fig. 1. From now on, we do not always write the time dependence of the coherent state labels explicitly in order to shorten the notation.

The influence of the dissipation is contained in the term  $\xi$  with

$$\begin{aligned}
i\dot{\xi} &= \gamma (2z_0 z_1^* - (|z_0|^2 + |z_1|^2)) \\
&= -\gamma |z_1 - z_0|^2 + i\gamma |z_1| |z_0| \sin(\theta_1 - \theta_0),
\end{aligned}$$

where the phases  $\theta_j$  are defined by  $z_j = |z_j| e^{i\theta_j}$ . Note that  $\xi$  consists of a real as well as of an imaginary part. In summary, an initial state which is in a superposition of spin states

$$\rho(0) = \begin{pmatrix} |a|^2 & ab^* \\ a^*b & |b|^2 \end{pmatrix} \otimes |z(0)\rangle\langle z(0)|,$$

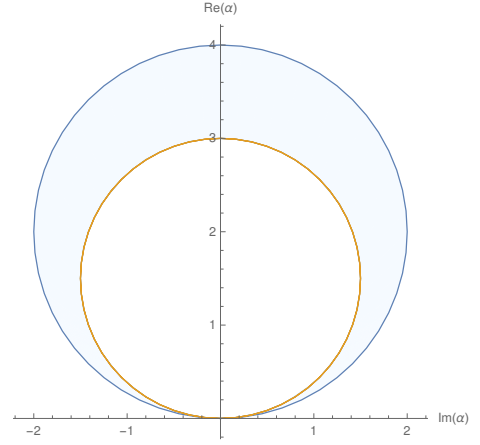


Figure 1. (color online) In the isolated case the relative phase between two cyclic evolutions is proportional to the difference of the swept phase space area in the interaction picture.

will be transformed into the following state after the cyclic evolution:

$$\rho(T) = \begin{pmatrix} |a|^2 & ab^* e^{i\varphi_{\text{isol}} + i\xi} \\ a^* b e^{-i\varphi_{\text{isol}} - i\xi} & |b|^2 \end{pmatrix} \otimes |z(0)\rangle\langle z(0)|.$$

This shows that for  $\gamma \neq 0$  the damping results in an additional real term  $\eta = \gamma \int_0^T |z_1 - z_0|^2 dt$  in the exponent which does only depend on the damping strength  $\gamma$  and the difference of the amplitudes of the paths. This real term leads to a dephasing of the spin state by diminishing the off-diagonal elements of the density matrix. We will therefore refer to it as dephasing term from now on.

We can also see a new phase term  $\varphi_L = \gamma \int_0^T |z_1| |z_0| \sin(\theta_1 - \theta_0) dt$  which depends on the absolute values of  $z_0$  and  $z_1$ . The integral over this term can vanish for sufficiently symmetrical  $z_j(t)$  (e.g. if  $z_j(t) = z_j(T-t)$ ) with  $j \in \{0, 1\}$  or if  $z_1$  or  $z_0$  is in the ground state during the entire operation. In Sec. IV we will see that the 2-qubit phase gates proposed in [14, 16] and realized in [10] do indeed have the latter property which means that even with damping the phases produced by those phase gates are still only determined by the respective areas. The dephasing term can, however, only vanish if  $f_1 = f_0$  which implies that there is no relative phase as well. We can also conclude that the dephasing is stronger for higher energies of the particle which means it is especially relevant for short operation times as we will see in Sec. IV A.

## B. Consequences for the path

We have seen in the previous section how the damping results in additional phase terms. However, from Eq. (14) it is clear that the damping alters the path as well. Therefore, the paths which are closed in the isolated

case are no longer closed in the damped case. It is a natural question to ask which forces  $\tilde{f}_j(t) = f_j(t)e^{i\omega t}$  can be used to achieve the cyclical evolution ( $z_j(0) = z_j(T)$ ) in the damped case and whether some of those forces should be used preferably because they minimize the dephasing term. First we note that it is not possible to completely compensate the effects of the damping by applying some sophisticated force  $f_c$ . This can be seen from Eq. (14), since the isolated dynamics of a coherent state is described by  $\dot{z}_j = 0$ , such a force would need to satisfy  $\tilde{f} = e^{i\omega t} f_c(t) = \text{const}$ , which is impossible for real  $f_c(t)$ .

To determine the effects of a force  $f_j(t)$  on the path  $z_j(t)$  we have to solve Eq. (14). This leads to the solution

$$\begin{aligned} z_j(t) &= z_{j,\text{hom}} + z_{j,\text{inhom}} \\ &= z_j(0)e^{-\gamma t} + \int_0^t \frac{-i}{\hbar} \tilde{f}_j e^{-\gamma(t-\tau)} d\tau. \end{aligned} \quad (24)$$

We can therefore conclude that in order to achieve the cyclic dynamics  $z_j(0) = z_j(T)$  we need the forces to satisfy

$$z_j(0) (e^{\gamma T} - 1) = \int_0^T f_j(\tau) e^{i\omega\tau} e^{\gamma\tau} d\tau. \quad (25)$$

The equation shows explicitly that for  $\gamma \neq 0$  the condition depends on the initial state  $z_j(0)$ . This means that in contrast to the undamped case where  $f_j$  would always lead to closed trajectories it now only works for a specific initial condition  $z_j(0)$ . The fault tolerance of a quantum phase gate towards the initial motional state is therefore lost in the damped case.

An interesting observation at this point is that if we consider  $z_j(0) = 0$ , we can derive forces  $f_d$  which return  $z_j$  to the ground state after time  $T$  in the damped case from the forces  $f_{\text{nd}}$  which accomplish this in the undamped case by using the formula

$$f_d = f_{\text{nd}} \cdot e^{-\gamma t}. \quad (26)$$

We will use this link between the damped and the undamped scenarios in the next section to generalize an already existing protocol for 2-qubit phase gate to account for dissipative effects.

For an experimental realization it is desirable to minimize the dephasing term for a given relative phase. To examine how this can be done we want to consider the case  $f_0(t) = 0$  and  $|z_j(0)\rangle = |0\rangle$  for the sake of simplicity. This means that  $|z_0\rangle$  is the ground state at all times and we only need to discuss the dynamics of  $|z_1\rangle$ . These simplifications are well justified because in an experimental setup the ground state can be prepared initially and an additional force  $f_0$  does not bring any benefits but just makes the computations more complex. We can then derive simple expressions for the phase and dephasing terms after time  $T$  from Eq. (23) if we write  $z_1 = r(t)e^{i\theta(t)}$  (in the following equations we have omitted the time depen-

dence of  $r$  and  $\theta$ )

$$\begin{aligned} \int_0^T z_1^* \dot{z}_1 dt &= \int_0^T r e^{-i\theta} (\dot{r} e^{i\theta} + i r \dot{\theta} e^{i\theta}) dt \\ &= \int_0^T r \dot{r} dt + i \int_0^T \dot{\theta} r^2 dt. \end{aligned}$$

Since  $z_1(0) = z_1(T)$  we can see that the first integral vanishes by integrating by parts and we are left with the following expression for the phase:

$$\varphi_{\text{isol}} = \int_0^T \dot{\theta} r^2 dt, \quad \varphi_L = 0. \quad (27)$$

In this case,  $\varphi_L = 0$  because  $z_0 = 0$  at all times. For the dephasing term we find

$$\eta = \gamma \int_0^T r^2 dt. \quad (28)$$

We can see that the easiest way to minimize the dephasing for a given relative phase is to make  $\dot{\theta}$  as large as possible. This result also makes intuitive sense since if the path goes around the origin multiple times (large  $\dot{\theta}$ ) it needs a smaller amplitude (which results in less dephasing) in order to sweep over the same area. Since  $\theta$  corresponds to the interaction picture it is affected by the frequency  $\omega$  of the harmonic oscillator.

Fig. 2 displays the paths  $z_1(t)$  which are generated by forces of the form  $f_1 = e^{-\gamma t} \sin(\Omega t)$  and  $f_0 = 0$  (see Eq. (14)). The paths (a) and (b) correspond to the isolated case with  $\gamma = 0$  whereas  $\gamma > 0$  for the paths (c) and (d). The exact parameters used in this numerical simulation were  $\Omega = 2$  MHz for the frequency of the driving force in all trajectories,  $\omega = 2\Omega$  for the frequency of the harmonic trap in trajectories (a) and (c) and  $\omega = 4\Omega$  for (b) and (d). The damping constant for paths (c) and (d) was set to  $\gamma/\Omega = 0.2$ . We can see how the upper two paths are symmetrical with respect to the imaginary axis. As shown in [14] this implies that the phase does not change (in first order) if the force is subjected to a homogeneous, small constant offset  $f \mapsto f + \delta f$  in the  $\gamma = 0$  case. In contrast, the paths for  $\gamma \neq 0$  are no longer symmetrical. However whether the path is symmetric or not depends on the force. In the next section we therefore want to investigate how the robustness can be maintained in the damped case by constructing forces differently compared to Eq. (26).

### C. Consequences for the robustness

At first we want to show how the condition for the robustness against small constant offsets of the force  $f \mapsto f + \delta f$  reads in the dissipative case studied here.

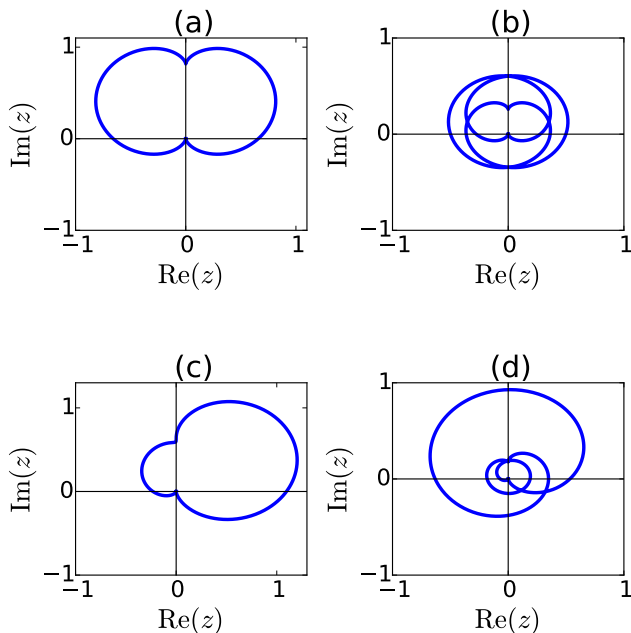


Figure 2. (color online) Path of  $z_1$  in the complex plane when using the force  $f(t) = e^{-\gamma t} \sin(\Omega t)$ . All paths were normalized to produce a phase of  $\pi$ . The paths in the upper row (a,b) were simulated without damping, whereas damping was included for the paths in the lower row (c,d) without changing the frequency of the trap or the driving force. The paths in the right column are simulated in a trap with a higher frequency and result in less dephasing although they produce the same phase compared to the left column.

According to Eq. (22) with  $z_0 = 0$ ,

$$\begin{aligned} \varphi_{\text{isol}} &= \int_0^T \text{Im}(\dot{z}_1 z_1^*) dt \\ &= \frac{-1}{\hbar} \int_0^T \text{Re}(z_1^S f_1) dt, \end{aligned}$$

where we used Eq. (14) and  $z_1^S = e^{-i\omega t} z_1$  is the path in the Schrödinger picture. Therefore the offset to the phase in first order becomes

$$\delta\varphi_{\text{isol}} = \frac{-\delta f}{\hbar} \int_0^T \text{Re}(z_1^S) dt \stackrel{!}{=} 0.$$

This result is identical to the one in the isolated case found in [14]. By inserting Eq. (24), assuming  $z_1(0) = 0$  and integrating by parts we can express this as a condition for the force

$$0 = \int_0^T f(t) dt. \quad (29)$$

Together with the condition for a cyclic evolution, Eq. (25), we therefore have a set of conditions that for

$z_j(0) = 0$  may be seen as orthogonality conditions for  $f(t)$

$$f(t) \perp \{e^{\gamma t} \sin(\omega t), e^{\gamma t} \cos(\omega t), 1\} =: \mathcal{C}. \quad (30)$$

This means that we can construct forces to suit our needs by a Gram-Schmidt procedure. It is useful to orthogonalize the set  $\mathcal{C}$  and then do one more orthogonalizing step for the arbitrary function  $g$  which will then become orthogonal to the set  $\mathcal{C}$ . This method makes it possible to construct a plethora of forces which will leave the phase unchanged under a small constant offset  $\delta f$  and produce a cyclic evolution. By superposing many of such forces one can then ensure to meet further demands like e.g.  $f(0) = f(T) = 0$ .

We can conclude that it is possible to maintain the robustness of the phase gate against small constant offsets of the force  $f \mapsto f + \delta f$  in the damped case. However as we have seen in the previous section (Eq. (25)) the gate loses its resistance against fluctuations in the initial motional state.

#### IV. APPLICATION TO 2-QUBIT PHASE GATES

In this section we want to show how the relations we found in the previous sections apply to two-qubit phase gates which have been realized in [10, 18]. These two-qubit gates consist of two ions in a harmonic trap potential which experience a force that depends on the internal state ( $|\uparrow\rangle$  or  $|\downarrow\rangle$ ) of the ion. As shown in [14], the Hamiltonian of such a system can be written as

$$\begin{aligned} H_{\text{tot}} &= H_+ + H_-, \\ H_{\pm} &= \frac{p_{\pm}^2}{2} + \frac{1}{2} \Omega_{\pm}^2 x_{\pm}^2 + f_{\pm} x_{\pm}. \end{aligned} \quad (31)$$

Here,  $H_+$  describes an oscillation of a stretch mode where the displacement from the equilibrium position of the two ions are equal but in opposite directions and  $H_-$  describes an oscillation of the center-of-mass mode where the displacement of the ions is identical.  $x_{\pm}$  are mass weighted normal mode coordinates which for equal mass ions take the form

$$x_{\pm} = \sqrt{m}((x_1 - x_1^{(0)}) \mp (x_2 - x_2^{(0)})).$$

Here,  $x_i$  is the position operator for ion  $i$ ,  $x_i^{(0)}$  is the equilibrium position of ion  $i$  and the canonically conjugate momentum operators are  $p_{\pm} = -i\hbar\partial/\partial x_{\pm}$ .

Note that here we ignored a term in  $H_{\text{tot}}$  which is proportional to the difference of the forces experienced by the two ions. This (purely time dependent) term will therefore lead to additional phases for certain configurations. Similar to Eq. (30) we will however later (see Eq.(39)) present a way to construct forces which satisfy  $\int_0^T f dt = 0$  so that this phase will vanish. A more detailed derivation of the Hamiltonian and discussion of the purely time dependent term can be found in [14].

If the forces on the two ions take the form  $F_j = F(t)\sigma_j^z$  one can derive the following values for the force in the interaction picture  $\tilde{f}_\pm$

$$\begin{aligned}\tilde{f}_+(P) &= \tilde{f}_-(A) = 0, \\ \tilde{f}_-(\uparrow\uparrow) &= -2F/\sqrt{2m}e^{i\Omega_-t}, \\ \tilde{f}_+(\uparrow\downarrow) &= -2F/\sqrt{2m}e^{i\Omega_+t}, \\ \tilde{f}_-(\downarrow\downarrow) &= 2F/\sqrt{2m}e^{i\Omega_-t}, \\ \tilde{f}_+(\downarrow\uparrow) &= 2F/\sqrt{2m}e^{i\Omega_+t},\end{aligned}\quad (32)$$

where  $P \in \{\uparrow\uparrow, \downarrow\downarrow\}$  denotes parallel and  $A \in \{\uparrow\downarrow, \downarrow\uparrow\}$  anti-parallel spin combinations. This type of force can be realized by off resonant lasers in the Lamb-Dicke regime [26]. For the optimization of the functional form of the force see [14]. Frequencies  $\Omega_\pm$  are defined as  $\Omega_+ = \sqrt{3}\omega$  and  $\Omega_- = \omega$  [14]. We can bring the Hamiltonian in the same form as in the previous section by introducing creation and annihilation operators for the stretch and center-of-mass mode  $a_\pm, a_\pm^\dagger$  and switching to an interaction picture

$$\begin{aligned}|\Psi_I\rangle &= e^{-iH_0t/\hbar}|\Psi\rangle, \\ H_0 &= \hbar\Omega_+(a_+^\dagger a_+ + \frac{1}{2}) + \hbar\Omega_-(a_-^\dagger a_- + \frac{1}{2}).\end{aligned}\quad (33)$$

The Hamiltonian then reduces to

$$\begin{aligned}\tilde{V} &= \tilde{f}_+^* a_+ + \tilde{f}_+ a_+^\dagger + \tilde{f}_-^* a_- + \tilde{f}_- a_-^\dagger \\ &= \tilde{V}_+ + \tilde{V}_-.\end{aligned}\quad (34)$$

To model the damping we can introduce two Lindblad terms similar to Eq. (9). We assume identical damping rates  $\gamma$  since all degrees of freedom couple to the same bath which we assume to have a flat spectral density on the relevant frequency scale. We then find in the interaction picture

$$\begin{aligned}\dot{\rho} &= \mathcal{L}_+[\rho] + \mathcal{L}_-[\rho], \\ \mathcal{L}_\pm &:= \frac{-i}{\hbar}[\tilde{V}_\pm, \rho] + \gamma \left( 2a_\pm \rho a_\pm^\dagger - a_\pm^\dagger a_\pm \rho - \rho a_\pm^\dagger a_\pm \right).\end{aligned}\quad (35)$$

We can see that the  $\mathcal{L}_\pm$  only act on one of the two modes and are of the same form as the right hand side of Eq. (9). Therefore the two modes  $+, -$  are not coupled by Eq. (35) and we can reuse the results from the previous Sec. III to determine the evolution of an initial state that is in a superposition of spin states and in a coherent motional state

$$\rho(0) = \begin{pmatrix} |a|^2 & ab^* \\ a^*b & |b|^2 \end{pmatrix} \otimes |z_+(0)\rangle\langle z_+(0)| \otimes |z_-(0)\rangle\langle z_-(0)|.$$

The coherent motional state evolves according to

$$\dot{z}_\pm^j + \gamma z_\pm^j = \frac{1}{i\hbar} \tilde{f}_\pm(j), \quad (36)$$

where the internal degrees of freedom are given by  $j$  and oscillation in the stretch and center-of-mass mode is described by  $z_+^j$  and  $z_-^j$  respectively. The forces  $\tilde{f}_\pm(j)$  are

given in Eq. (32). Furthermore, we can observe that Eq. (35) is of the form of Eq. (15) which means that we can apply the results from Sec. III A to calculate the phase and dephasing which arise during a cyclic evolution:

$$\varphi(T) = \varphi_{\text{isol}} + \xi, \quad (37)$$

where

$$\begin{aligned}\varphi_{\text{isol}} &= 2(A_+^1 + A_-^1 - A_+^0 - A_-^0), \\ \xi &= \gamma \int_0^T d_+(\tau) + d_-(\tau) d\tau, \\ d_\pm &= i|z_\pm^1 - z_\pm^0|^2 + |z_\pm^0||z_\pm^1| \sin(\theta_\pm^1 - \theta_\pm^0).\end{aligned}$$

We see that  $\varphi_{\text{isol}} = \varphi_g + \varphi_d$  is proportional to the areas swept in the stretch and center-of-mass modes of oscillation  $A_+$  and  $A_-$ , respectively, and it is identical to the phase of the isolated evolution ( $\gamma = 0$ ). Because of the symmetries of the forces described in Eq. (32),  $\varphi_{\text{isol}}$  is only nonzero if 0 is a parallel and 1 an anti-parallel spin combination or vice versa. The  $\xi$  term originates from the Lindblad operators and since  $\text{Im}(\xi) \neq 0$  it will result in dephasing equivalently to the one ion case discussed in Sec. III A. However, if the evolution starts in the ground state either  $z_\pm^0$  or  $z_\pm^1$  will remain in the ground state for the entire operation because of Eq. (32). Therefore  $\text{Re}(\xi)$  will always be zero which means that the phase depends only on the difference of the swept phase space areas like in the undamped case studied in [14].

Since the equations (36) for the evolution of  $z$  are identical to the one ion case, Eq. (26) still holds true and we can easily generalize the force  $F_{\text{nd}}$  constructed in [14] to the damped oscillator:

$$F(t) = \kappa e^{-\gamma t} \cdot F_{\text{nd}}. \quad (38)$$

According to Eq. (24) this means for the damped path

$$z_d = \kappa e^{-\gamma t} z_{\text{nd}}.$$

Here we introduced two correction factors  $\kappa$  and  $e^{-\gamma t}$  to the original force for the undamped case.  $\kappa$  is a constant to compensate for the smaller area due to the damping and it therefore ensures that the phase (which corresponds to the area) stays the same. The exponential factor ensures that  $z$  returns to the ground state after time  $T$ .

It would also be possible to construct forces via the Gram-Schmidt process described in Sec. III C to maintain the resistance against small constant offsets of the force. Since these forces now have to produce closed paths in both modes there are more orthogonality conditions

$$\begin{aligned}f \perp \{e^{\gamma t} \sin(\Omega_+ t), e^{\gamma t} \cos(\Omega_+ t), \\ e^{\gamma t} \sin(\Omega_- t), e^{\gamma t} \cos(\Omega_- t), 1\},\end{aligned}\quad (39)$$

but the method of constructing  $f$  stays the same. For the next section we will nevertheless stick to Eq. (38)

since the resulting forces are less complex and sufficient for discussing the impact on the fidelity.

The paths of the resulting  $z_{\pm}$  with and without damping and under the influence of different forces are shown in Fig. 3. The plots (a), (b) and (c) are in the interaction picture whereas the plot (d) is in the Schrödinger picture. The parameters for trajectory (a) were chosen identically to [14]:  $T = 0.8 \mu\text{s}$ ,  $\omega/2\pi = 2 \text{ MHz}$  and  $\gamma/\omega = 0$ . The trajectory (b) corresponds to the same force and parameters as trajectory (a) but now with a damping  $\gamma/\omega = 0.1$ . We can see how the path is no longer closed and that the area decreased as well. In the plot (c) we used the same damping and parameters as in (b) but with the adjusted force (38). Now the paths are closed again and the area difference is identical to (a). The plot (d) shows the trajectory for a shorter operation time  $T = 0.3\mu\text{s}$  in the Schrödinger picture. It is important to note that the ticks are different for this plot because the trajectory has a much greater amplitude. The intuitive reason for this is that the particle needs a large momentum to complete the loop in a shorter time, the trajectory is therefore stretched out in  $p \propto \text{Im}(z^S)$  direction. This illustrates that shorter operation times come with the trade-off of more dephasing (see Sec. IV A and Fig. 4).

### A. Influence of damping on the fidelity

The fidelity measures the overlap of the final state  $\rho_f$  with the desired state  $|\Psi_d\rangle$

$$\mathcal{F} = \langle \Psi_d | \rho_f | \Psi_d \rangle.$$

Since we want to implement a two qubit phase gate our desired state  $|\Psi_d\rangle$  is

$$|\Psi_d\rangle = ae^{i\varphi_{\text{isol}}} |P\rangle + b|A\rangle,$$

with  $|a|^2 + |b|^2 = 1$ .  $P$  and  $A$  denote an arbitrary parallel and anti-parallel spin combination (e.g.  $P = \uparrow\uparrow$  and  $A = \uparrow\downarrow$ ). The final (spin-) state (in the basis  $\{|P\rangle, |A\rangle\}$ ) after the cyclic evolution is

$$\rho_f = \begin{pmatrix} |a|^2 & ab^* e^{i\varphi_{\text{isol}} - \Gamma} \\ a^* b e^{-i\varphi_{\text{isol}} - \Gamma} & |b|^2 \end{pmatrix},$$

where

$$\Gamma = \gamma \int_0^T (|z_+(A)|^2 + |z_-(P)|^2) dt. \quad (40)$$

We can calculate the fidelity as

$$\mathcal{F} \geq \frac{1 + e^{-\Gamma}}{2}. \quad (41)$$

The lower bound of the inequality above is reached if the prefactors satisfy  $a = b = 1/\sqrt{2}$ .

Figure 4 shows the maximal infidelity  $1 - \mathcal{F}$  and phase difference  $\Delta\varphi = 2(\varphi(A) - \varphi(P))$  for different  $\gamma$  and  $T$ .

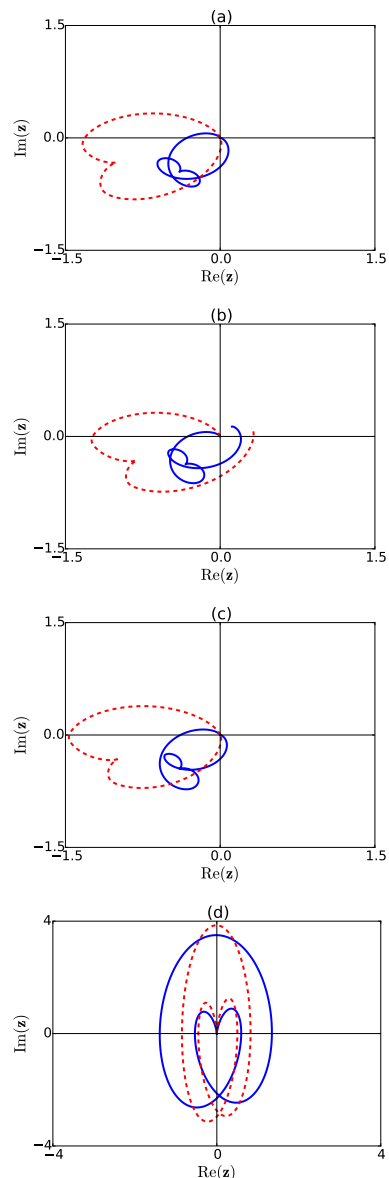


Figure 3. (color online) Figure (a), (b) and (c) show paths of  $z_+(\uparrow\downarrow)$  (solid blue line) and  $z_-(\uparrow\uparrow)$  (dashed red line) in the interaction picture. Figure (d) shows paths in the Schrödinger picture. Plot (a) corresponds to one of the cases studied by [14]. The damping was set to zero and the other parameters were chosen as  $T = 0.8\mu\text{s}$ ,  $\omega/(2\pi) = 2 \text{ MHz}$ . Plot (b) shows a path generated by the same force but in the presence of fairly strong damping  $\gamma = 0.1\omega$ . We can clearly see how the paths are no longer closed which would lead to a loss of fidelity. This can be fixed by applying the force (38) which accounts for the damping as shown in (c). Plot (d) shows the trajectory for a shorter operation time  $T = 0.3\mu\text{s}$  in the Schrödinger picture. Note that this trajectory has a much greater amplitude which leads to more dephasing. Because of that, we can conclude that shorter operation times come with the trade-off of more dephasing (see Fig. 4).



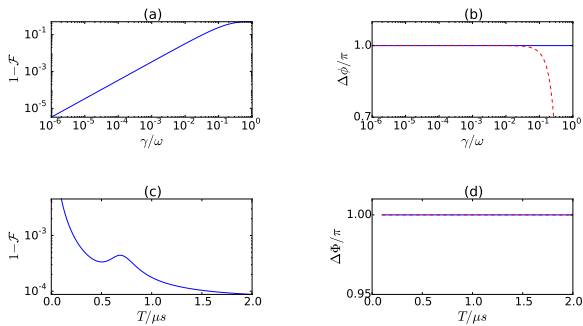


Figure 4. (color online) The upper two plots show the maximum infidelity (a) and phase (b)  $\Delta\varphi = 2(\varphi(A) - \varphi(P))$  for different values of  $\gamma$  with constant  $T = 0.8\mu\text{s}$  and the plots (c) and (d) show these values for different operation times and constant  $\gamma/\omega = 10^{-4}$ . The solid blue line in (b) and (d) represent the phase difference of trajectories which result from the force (38) which accounts for the damping and the dashed red lines represent the phase difference of trajectories which result from the original force.

In (a) and (b) the operation time was chosen as constant  $T = 0.8\mu\text{s}$  whereas  $\gamma/\omega$  varied and in (c) and (d) we chose constant  $\gamma/\omega = 10^{-4}$  for varying  $T$ . The plots (b) and (d) show the phase difference for the force given in Eq. (38) which accounts for the damping (solid blue line) and for the original force (dashed red line). We can see that the force we constructed (blue line) correctly compensates for the phase whereas lack of compensation would lead to a drastic phase deviation for larger damping strengths. Different operation times do not affect the phase significantly for both forces because for  $\gamma/\omega = 10^{-4}$  the lost area is still marginal. For large  $\gamma$  the curve in (a) goes towards 1/2 apart from that the infidelity is roughly in the same order of magnitude as  $\gamma/\omega$ . In the plot (c) it is demonstrated that short operation times  $T$  lead to a higher infidelity, because the forces needed to achieve the desired phase result in a higher amplitude  $|z|$  and therefore in a larger  $\Gamma$  (see Fig. 3 (d)). The bump in figure (c) comes from our choice of the path and has no other physical meaning. We can compare these infidelities which are roughly of the order of  $\gamma/\omega$  to infidelities from different sources studied by [14]. The infidelity caused by the anharmonic Coulomb repulsion is below  $10^{-4}$  whereas the infidelity caused by considering the correct sinusoidal form of the force  $F(x, t) = F(t) \cdot \sin(kx)$  is in between  $10^{-5}$  and 0.1 depending on the operation time.

## V. FINITE TEMPERATURE EFFECTS

In section II B we outlined how the effects of finite temperature can be taken into account by using a noisy force equal to  $\tilde{f}_j(t) + \sqrt{2\gamma\bar{n}\hbar}\chi(t)$ , where  $\chi(t)$  is a complex valued Gaussian white noise process. In this section we show how the previous results can be extended to include

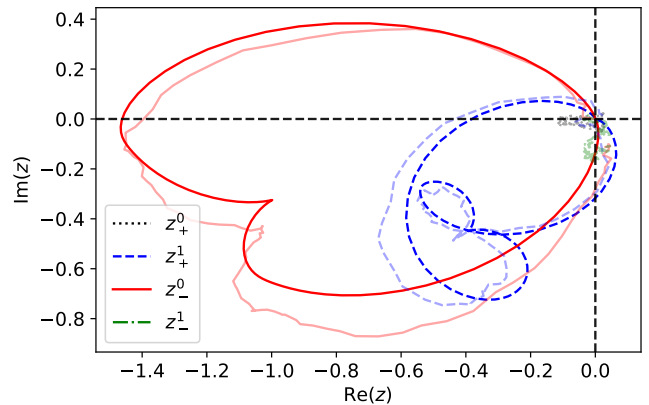


Figure 5. (color online) Comparison of trajectories between finite temperature ( $\gamma\bar{n}T \approx 0.03$ ) (light colors) and zero temperature (dark colors). Thermal fluctuations are clearly visible around the zero temperature paths  $z_+^1, z_-^0$ . Moreover  $z_+^0, z_-^1$  fluctuate around the ground state  $(0, 0)$  when temperature is non-zero, leading to imperfections in the phase gate implementation. Other parameters are as in Fig. 3 c).

finite temperature effects and what impact these effects have on the fidelity of a two-qubit phase gate.

We begin with a stochastic GKSL-type master equation that describes the influence of a finite temperature heat bath coupled to the trapped ions implementing the two qubit phase gate. We model the effect of the heat bath by equal strength but independent damping of both vibration modes ( $a_{\pm}$ ) and by independent thermal noise processes affecting both modes ( $\chi_{\pm}(t)$ )

$$\begin{aligned} \dot{\rho}_{\chi} &= \mathcal{L}_{\chi,+}[\rho_{\chi}] + \mathcal{L}_{\chi,-}[\rho_{\chi}], \\ \mathcal{L}_{\chi,\pm}[\rho] &= \frac{-i}{\hbar} [\tilde{V}_{\chi,\pm}, \rho] + \gamma \left( 2a_{\pm}\rho a_{\pm}^{\dagger} - a_{\pm}^{\dagger}a_{\pm}\rho - \rho a_{\pm}^{\dagger}a_{\pm} \right), \\ \tilde{V}_{\chi,\pm} &= (\tilde{f}_{\pm}^* + \sqrt{2\gamma\bar{n}\hbar}\chi_{\pm}^*(t))a_{\pm} + (\tilde{f}_{\pm} + \sqrt{2\gamma\bar{n}\hbar}\chi_{\pm}(t))a_{\pm}^{\dagger} \\ \rho &= \langle \rho_{\chi} \rangle. \end{aligned} \quad (42)$$

In this form the equation is almost identical to Eq. (35) with the small difference that the thermal noise has been added to the deterministic driving force. The solution  $\rho_{\xi}$  is similar to the zero temperature case, with the addition of the random thermal process. Solution can be expressed in terms of coherent states, whose labels satisfy

$$\dot{z}_{\pm}^j + \gamma z_{\pm}^j = \frac{1}{i\hbar} \left( \tilde{f}_{\pm}(j) + \sqrt{2\gamma\bar{n}\hbar}\chi_{\pm} \right). \quad (43)$$

However an important difference is that due to the noise the path can no longer be closed reliably by choosing an appropriate force. As can be seen in Fig. 5, the thermal noise causes fluctuations around the paths driven by deterministic force ( $z_+^1, z_-^0$ ) and the non-driven paths ( $z_+^0, z_-^1$ ) are no longer stationary but fluctuate around the ground state.

### A. Fidelity in the finite temperature case

One important question is how the fidelity of the phase gate is affected by the thermal noise and whether the compensation strategy suggested in III B still improves this fidelity. In this section we seek to answer this question.

As in section IV A the fidelity is defined as

$$\mathcal{F} = \langle \Psi_d | \rho(T) | \Psi_d \rangle.$$

Since in the finite temperature case the density operator is given as an average  $\rho = \langle \rho_\chi \rangle$  the fidelity can be obtained by averaging as well,

$$\mathcal{F} = \langle \langle \Psi_d | \rho_\chi(T) | \Psi_d \rangle \rangle.$$

We will proceed to first evaluate the fidelity for a general  $\rho_\chi(T)$  and then take the average over the stochastic processes  $\chi_\pm(t)$ .

We again consider the overlap with the target state  $|\Psi_d\rangle = ae^{i\varphi_{\text{isol}}}|P\rangle + b|A\rangle$  and choose  $a = b = 1/\sqrt{2}$ . Other choices for the prefactors will lead to higher fidelity as discussed in Sec. IV A. The fidelity of any  $\rho_\chi$  after the phase gate operation is given as

$$\begin{aligned} \mathcal{F} = & \frac{1}{4} (\exp(-(|z_-^1|^2 + |z_+^1|^2)) + \exp(-(|z_-^0|^2 + |z_+^0|^2))) \\ & + 2 \operatorname{Re}(e^{-i\Delta\varphi - \Gamma - \frac{1}{2}(|z_-^1|^2 + |z_+^1|^2 + |z_-^0|^2 + |z_+^0|^2)}), \end{aligned} \quad (44)$$

$$\Gamma = \gamma \int_0^T |z_+^1(\tau) - z_+^0(\tau)|^2 + |z_-^1(\tau) - z_-^0(\tau)|^2 d\tau,$$

$$\Delta\varphi = \varphi(T) - \varphi_{\text{isol}}.$$

All quantities in the expression for  $\mathcal{F}$  are evaluated at time  $T$ , that is, at the end of the phase gate operation. In the expression one can identify the three possible causes for fidelity-loss:

1. The terms  $\propto \exp(|z_\pm^j(T)|^2)$  arise when the path is not closed, which means that  $z(T) \neq 0$ .
2. The term  $\exp(-i\Delta\varphi)$  occurs when  $\varphi(T) \neq \varphi_{\text{isol}}$ ,
3. and the term  $\exp(-\Gamma)$  describes decoherence, which is induced by the damping and can not be prevented.

In the zero temperature case we could close the path and restore the phase of the isolated case. Therefore only the decoherence was contributing to a fidelity loss and the formula reduced to Eq. (41). For finite temperature this is no longer the case and we therefore have to work with the full expression for  $\mathcal{F}$ . We have plotted the average infidelity as a function of  $\gamma\bar{n}T$  over 5000 realizations in Fig. 6 (solid line). We checked that our result coincide with directly solving the master equation (9) (not shown in the Figure). The other parameters are as in Fig. 3

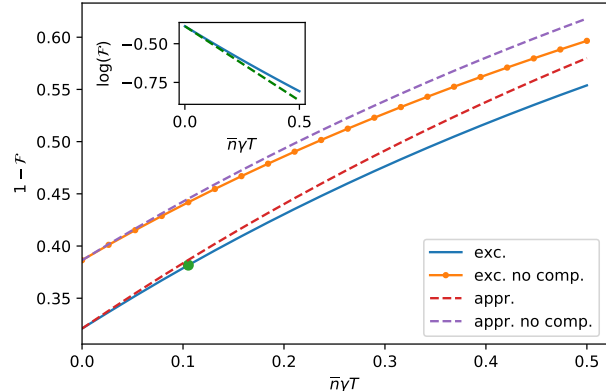


Figure 6. (color online) Infidelity with respect to thermal fluctuations and the logarithm of fidelity with compensation (inset). Compensated force clearly improves the fidelity even in the presence of thermal fluctuations. When  $\gamma\bar{n}T \approx 0.1$  then  $1 - \mathcal{F} \approx 0.38$  (dot), which corresponds to approximately 19% increase compared to the zero temperature. Fidelity decreases sub-exponentially as a function  $\gamma\bar{n}T$ , as can be seen from the inset. Dashed lines corresponds to a second order cumulant expansion of the fidelity. Other parameters are as in Fig. 3 c), except  $\gamma/\omega = 0.2$ .

c), except  $\gamma/\omega = 0.2$ . We see that the compensation strategy improves the fidelity even at finite temperatures. The reason is that it still increases the average overlap of the final state and the ground state. We note, however, that the importance of this effect decreases as  $\bar{n}/(\gamma T)$  increases. When  $\gamma\bar{n}T \approx 0.1$  (dot)  $\mathcal{F} \approx 0.61$  and given the values  $T = 0.3\mu\text{s}$ , and  $\gamma/\omega = 0.2$  and  $\omega/2\pi = 2$  MHz, the average thermal photon number  $\bar{n} \approx 2.7$ . This corresponds to a temperature of about 0.3 mK (we evaluate  $\bar{n}$  at  $\omega$ ). These temperatures are within the range of current experimental capabilities, see for example [27]. In the appendix A we evaluate the  $\chi$  dependence of the fidelity. We use a cumulant expansion to find an approximate analytical expression for the average fidelity. This approximation is plotted in Fig. 6 (dashed line)[28]. The inset shows that our approximation gives the first order correction in  $\gamma\bar{n}T$  to the zero temperature result. This approximation is motivated by the fact that for current ion traps the operation time  $T$  is much faster than the coherence time  $1/(\bar{n}\gamma)$ [18, 29]. Our scenario is in the range  $\bar{n}\gamma \sim 10^{-1}T$  and as we can see, the approximation nicely captures the finite temperature effects on the fidelity in this regime. The rather complicated approximate expression can be found in the appendix.

## VI. SUMMARY AND OUTLOOK

We examined how phase gates based on the geometrical phases of driven trapped ions behave under dissipa-

tion. We used forces which depend on an internal state of the trapped ion in order to construct relative phases which show up in the density operator. We then showed that in the special case of a GKSL-type evolution with closed phase space paths admitting pure state solutions the total phase will always have an additional third contribution beyond dynamical- and geometric phases due to dissipation

$$\begin{aligned}\varphi &= \varphi_d + \varphi_g + \xi, \\ \xi &= \varphi_L + i\eta.\end{aligned}$$

This third contribution will in general be complex and can be directly related to the Lindblad operators. Applied to the harmonic oscillator this means that the damping results in a new additional phase that can however vanish for certain special cases. More severely, dephasing occurs which cannot be avoided and depends on the amplitude of the oscillation and the damping strength. We applied our results obtained for a single trapped ion to a two-qubit phase gate proposed in [14] which is based on two trapped ions. We found that in the presence of damping the phase produced by the gate depends on the area swept in the interaction picture alone, if the ion is in the ground state at the beginning of the operation. However due to the dephasing the fidelity of the gate is reduced. This loss of fidelity is especially noticeable for large damping strengths or short operation times. Furthermore, our calculations show how due to the damping the phase gate no longer operates independently of the initial motional state. On the other hand it is possible to maintain the robustness against small constant offsets of the force  $f \mapsto f + \delta f$  in the damped case by constructing the force using a Gram-Schmidt procedure that also ensures that the force produces a closed phase space path evolution. We considered also finite temperature effects in order to assess the feasibility of this scheme. We conclude that this scheme could be soon within reach of current experimental techniques by reducing the operation time of the gate or by using colder ion traps, thus preventing the onset of thermal fluctuations.

To give fair assessment of the relevance of our results, we point out that at the moment two qubit gates are typically experimentally implemented under conditions where the motional state of the ion is rather heated than damped [5, 6]. However, our results predict improvement on the performance of the geometric phase gate if it would be implemented using buffer gas cooling scenario [27] where damping can be the main source for gate errors.

This work could be extended to more than two ions if the block structure of the Hamiltonian is kept and only independent decay processes are considered. In future work we will model the system from first principles in order to determine the validity of the phenomenological model presented and analyzed in this article.

## ACKNOWLEDGMENTS

The authors would like to thank Valentin Link for fruitful discussions and the anonymous Referees for valuable comments.

### Appendix A: Analyzing the phase of a dissipative time evolution

Since we assumed that the evolution can be described by a pure state we can construct two solutions to Eq. ((15)):

$$\begin{aligned}\rho_{00}(t) &= |0\rangle\langle 0| \otimes |\Psi_0(t)\rangle\langle\Psi_0(t)| \\ \rho_{11}(t) &= |1\rangle\langle 1| \otimes |\Psi_1(t)\rangle\langle\Psi_1(t)|.\end{aligned}$$

In order to determine the relative phase between those two states we examine the evolution of the superposition which means that we have a density operator of the form

$$\begin{aligned}\rho &= \rho_{00} + \rho_{01} + (\rho_{01})^\dagger + \rho_{11} \\ \rho_{01} &= e^{i\varphi(t)} |0\rangle\langle 1| \otimes |\Psi_0\rangle\langle\Psi_1|.\end{aligned}\quad (\text{A1})$$

We already know that  $\rho_{00}$  and  $\rho_{11}$  solve the equation so after inserting  $\rho$  into Eq. (15) we are left with

$$\begin{aligned}\dot{\rho}_{01} &= \frac{-i}{\hbar} [H, \rho_{01}] + [\rho_{01}] \\ \mathcal{L}[\rho_{01}] &= \sum_{l=1}^N L_l \rho_{01} L_l^\dagger - \frac{1}{2} \left( L_l^\dagger L_l \rho_{01} + \rho_{01} L_l^\dagger L_l \right).\end{aligned}\quad (\text{A2})$$

In analogy to [20] we can use (A1) and calculate

$$\begin{aligned}\dot{\rho}_{01} &= -i\dot{\varphi}\rho_{01} + e^{-i\varphi(t)} \frac{d}{dt} (|0\rangle\langle 1| \otimes |\Psi_0\rangle\langle\Psi_1|) \\ -\dot{\varphi} &= -i\langle\Psi_0| \left( \frac{d}{dt} |\Psi_0\rangle\langle\Psi_1| \right) |\Psi_1\rangle + ie^{-i\varphi} \langle\Psi_0|\dot{\rho}_{01}|\Psi_1\rangle.\end{aligned}\quad (\text{A4})$$

Since we want to determine  $\dot{\varphi}$  this leaves us with two terms to evaluate:

$$\langle\Psi_0| \left( \frac{d}{dt} |\Psi_0\rangle\langle\Psi_1| \right) |\Psi_1\rangle = \langle\Psi_0|\dot{\Psi}_0\rangle + \langle\dot{\Psi}_1|\Psi_1\rangle,$$

and

$$\begin{aligned}e^{-i\varphi(t)} \langle\Psi_0|\dot{\rho}_{01}|\Psi_1\rangle &= \frac{-ie^{-i\varphi}}{\hbar} (\langle\Psi_0|[H, \rho_{01}] + L[\rho_{01}]|\Psi_1\rangle) \\ &= \frac{-i}{\hbar} (\langle\Psi_0|H|\Psi_0\rangle - \langle\Psi_1|H|\Psi_1\rangle) \\ &\quad + \sum_{l=1}^N \langle\Psi_0|L_l|\Psi_0\rangle\langle\Psi_1|L_l^\dagger|\Psi_1\rangle \\ &\quad - \frac{1}{2} \left( \langle\Psi_0|L_l^\dagger L_l|\Psi_0\rangle + \langle\Psi_1|L_l^\dagger L_l|\Psi_1\rangle \right).\end{aligned}$$

This leads to the final result

$$-\frac{d\varphi}{dt} = -i(\langle\Psi_0|\partial_t|\Psi_0\rangle - \langle\Psi_1|\partial_t|\Psi_1\rangle) + \frac{1}{\hbar}(\langle H_0\rangle - \langle H_1\rangle) \\ + i\sum_{l=1}^N\langle\Psi_0|L_l|\Psi_0\rangle\langle\Psi_1|L_l^\dagger|\Psi_1\rangle \\ - \frac{1}{2}\left(\langle\Psi_0|L_l^\dagger L_l|\Psi_0\rangle + \langle\Psi_1|L_l^\dagger L_l|\Psi_1\rangle\right).$$

Here we also used that  $\langle\Psi|\dot{\Psi}\rangle$  is purely imaginary and therefore  $\langle\Psi|\dot{\Psi}\rangle = -\langle\dot{\Psi}|\Psi\rangle$ .

## Appendix B: Fidelity at finite temperature

In Sec. V we derived an expression for the fidelity of the gate for finite temperatures. Since this expression depends on the random noise  $\chi$  we have to take the average of  $\mathcal{F}$  over  $\chi$  in order to make meaningful predictions about the fidelity of the phase gate.

We will first take the averages of the terms  $\propto \exp(-|z_\pm^j(T)|^2)$  and later evaluate the average of the term  $\exp(-i\Delta\varphi - \Gamma - \frac{1}{2}(|z_-^1|^2 + |z_+^1|^2 + |z_-^0|^2 + |z_+^0|^2))$ .

In the finite temperature case the presence of noise leads to the following equation for  $z(t)$ :

$$z_\pm^j(t) = \frac{1}{i\hbar} \int_0^t (f_\pm^j + \sqrt{2\gamma\bar{n}\hbar}\chi_\pm) e^{i\Omega_\pm\tau - \gamma(t-\tau)} d\tau. \quad (\text{B1})$$

Note that there are two different uncorrelated noises  $\chi_\pm$  for the two different modes of oscillation (stretch and center of mass mode) that do however not depend on the internal states. Since the noise is just added to the force we can split  $z$  in two parts, where one part  $z_{\pm,f}^j(t)$  is under full control of the force (zero temperature path) and the second part  $z_{\pm,\chi}^j(t)$  is a fluctuation due to the noise.

$$z_\pm^j(t) = z_{\pm,f}^j(t) + z_{\pm,\chi}^j(t), \quad (\text{B2}) \\ z_{\pm,f}^j(t) = \frac{1}{i\hbar} \int_0^t f_\pm^j e^{i\Omega_\pm\tau - \gamma(t-\tau)} d\tau, \\ z_{\pm,\chi}^j(t) = \frac{1}{i\hbar} \int_0^t \sqrt{2\gamma\bar{n}\hbar}\chi_\pm e^{i\Omega_\pm\tau - \gamma(t-\tau)} d\tau.$$

Since  $z_{\pm,f}^j$  does not depend on  $\chi$  we arrive at

$$\langle \exp(-|z_\pm^j(T)|^2) \rangle = e^{-|z_{\pm,f}^j(T)|^2} \\ \times \langle \exp\left[-z_{\pm,f}^{j*}(T)z_{\pm,\chi}^j(T) - z_{\pm,f}^j(T)z_{\pm,\chi}^{j*}(T) - |z_{\pm,\chi}^j(T)|^2\right] \rangle \quad (\text{B3})$$

If we define

$$\mathcal{V}_\pm^j(\tau) = -z_{\pm,f}^{j*}(T) \frac{1}{i\hbar} \sqrt{2\gamma\bar{n}\hbar}\chi_\pm e^{i\Omega_\pm\tau - \gamma(T-\tau)} \\ - z_{\pm,f}^j(T) \frac{1}{-i\hbar} \sqrt{2\gamma\bar{n}\hbar}\chi_\pm^* e^{-i\Omega_\pm\tau - \gamma(T-\tau)} \\ - \int_0^T 2\gamma\bar{n}\chi_\pm(\tau)\chi_\pm^*(s) e^{i\Omega_\pm(\tau-s) - \gamma(T-\tau+T-s)} ds, \quad (\text{B4})$$

we can rewrite Eq. (B3) as

$$\langle e^{-|z_\pm^j(T)|^2} \rangle = e^{-|z_{\pm,f}^j(T)|^2} \langle e^{\int_0^T \mathcal{V}_\pm^j(\tau) d\tau} \rangle. \quad (\text{B5})$$

We now evaluate the average term by taking the cumulant expansion to 2nd order:

$$\langle e^{\int_0^T \mathcal{V}_\pm^j(t) dt} \rangle = e^{\int_0^T \langle \mathcal{V}_\pm^j(t) \rangle dt + \frac{1}{2} \int_0^T \int_0^T \langle \mathcal{V}_\pm^j(t_1)\mathcal{V}_\pm^j(t_2) \rangle dt_1 dt_2 + \dots}$$

Using the Gaussian nature of the processes  $\chi_\pm$  we get

$$\langle e^{-|z_\pm^j(T)|^2} \rangle \approx \exp\left[-\bar{n}(1 - e^{-2\gamma T}) - |z_{\pm,f}^j|^2(1 - \bar{n}(1 - e^{-2\gamma T})) + \frac{3}{2}(\bar{n}(1 - e^{-2\gamma T}))^2\right]. \quad (\text{B6})$$

From the result we can see that the finite temperature leads to additional decoherence which increases even further for  $z_{\pm,f}^j(T) \neq 0$ . Note that  $z_{\pm,f}^j(T) = 0$  when the path is closed in the zero temperature case. The third term in the expansion above is of the order  $(\gamma\bar{n}T)^2 = (T/\tau_d)^2$ . Since the coherence time  $\tau_d$  is much larger than the operation time for current ion-traps [18, 23] we will only keep terms in the first order of  $\gamma\bar{n}T$  from here on. We are now going to take a look at the average of the term

$$\langle e^{-i\Delta\varphi - \Gamma - \frac{1}{2}(|z_-^1|^2 + |z_+^1|^2 + |z_-^0|^2 + |z_+^0|^2)} \rangle. \quad (\text{B7})$$

At first one finds that  $\Gamma$  is actually independent of  $\chi$  since it is defined as the difference between two paths of different internal states (see Eq. (44)) and since the noise is independent of the internal state it cancels out. We then follow the same strategy as before and introduce a  $\mathcal{V}'(t)$  and approximate the exponential with a cumulant expansion

$$\mathcal{V}'(\tau) = -i\dot{\varphi}_\chi(\tau) + \frac{1}{2}(\mathcal{V}_-^1(\tau) + \mathcal{V}_+^1(\tau) + \mathcal{V}_-^0(\tau) + \mathcal{V}_+^0(\tau)).$$

Like the trajectory before we also split the phase into a part that is determined by the force alone  $\varphi_f$  and a part that depends on the noise  $\varphi_\chi$ :  $\varphi = \varphi_f + \varphi_\chi$ . With this definition we can write Eq. (B7) as

$$e^{-i(\varphi_f - \varphi_{\text{isol}}) - \Gamma - \frac{1}{2}(|z_{f,-}^1|^2 + |z_{f,+}^1|^2 + |z_{f,-}^0|^2 + |z_{f,+}^0|^2)} \langle e^{\int_0^T \mathcal{V}'(\tau) d\tau} \rangle.$$

We again take the cumulant expansion up to 2nd order and only keep terms up to first order of  $\gamma\bar{n}T$  to arrive at:

$$\begin{aligned}
& \langle \exp(-i\Delta\varphi - \Gamma - \frac{|z_-^1|^2 + |z_+^1|^2 + |z_-^0|^2 + |z_+^0|^2}{2}) \rangle \cong \exp \left[ -i(\varphi_f(T) - \varphi_{\text{isol}}) - \Gamma - 2\bar{n}(1 - e^{-2\gamma T}) \right. \\
& + \frac{\gamma\bar{n}}{\hbar} \text{Im} \left( \int_0^T dt_1 \int_0^{t_1} dt_2 \left( z_{-,f}^{1*}(t_2) \tilde{f}_-^1(t_1) + z_{+,f}^{0*}(t_2) \tilde{f}_+^0(t_1) \right) e^{-\gamma(T+t_1-2t_2)} \right) \\
& - \frac{\bar{n}}{\hbar^2} \text{Re} \left( \int_0^T dt_1 \int_0^{t_1} dt_2 \left( \tilde{f}_-^1(t_1) \tilde{f}_-^{1*}(t_2) + \tilde{f}_+^0(t_1) \tilde{f}_+^{0*}(t_2) \right) e^{-\gamma t_1} \sinh(\gamma t_2) \right) \\
& + \frac{\gamma\bar{n}}{2} \int_0^T dt_1 |z_{-,f}^1(t_1)|^2 + |z_{+,f}^0(t_1)|^2 + \frac{i\bar{n}}{\hbar} \text{Re} \left( \int_0^T dt_1 \left( z_{-,f}^1(T) \tilde{f}_-^1(t_1) - z_{+,f}^0(T) \tilde{f}_+^0(t_1) \right) e^{-\gamma T} \sinh(\gamma t_1) \right) \\
& \left. - \frac{|z_{-,f}^1(T)|^2 + |z_{+,f}^0(T)|^2}{2} (1 - \bar{n}(1 - e^{-2\gamma T})) \right]. \tag{B8}
\end{aligned}$$

With Eq. (B6), (B8) we can now express the average fidelity in first order of  $\bar{n}\gamma T$ , where we also expanded the exponentials of  $\gamma T$ :

$$\begin{aligned}
\langle \mathcal{F} \rangle & \cong \frac{\exp(-4\bar{n}\gamma T - |z_{-,f}^1(T)|^2(1 - 2\bar{n}\gamma T)) + \exp(-4\bar{n}\gamma T - |z_{+,f}^0(T)|^2(1 - 2\bar{n}\gamma T))}{4} \\
& + \frac{1}{2} \text{Re} \left[ \exp \left\{ -i(\varphi_f(T) - \varphi_{\text{isol}}) - \Gamma - 4\bar{n}\gamma T - \frac{\gamma\bar{n}}{2} \int_0^T dt_1 |z_{-,f}^1(t_1)|^2 + |z_{+,f}^0(t_1)|^2 \right. \right. \\
& + \frac{\gamma\bar{n}}{\hbar} \text{Im} \left( \int_0^T dt_1 \int_0^{t_1} dt_2 z_{+,f}^{0*}(t_2) \tilde{f}_+^0(t_1) + z_{-,f}^{1*}(t_2) \tilde{f}_-^1(t_1) \right) \\
& + \frac{i\gamma\bar{n}}{\hbar} \text{Re} \left( \int_0^T dt_1 \left( z_{-,f}^1(T) \tilde{f}_-^1(t_1) - z_{+,f}^0(T) \tilde{f}_+^0(t_1) \right) t_1 \right) \\
& - \frac{\gamma\bar{n}}{\hbar^2} \text{Re} \left( \int_0^T dt_1 \int_0^{t_1} dt_2 \left( \tilde{f}_-^1(t_1) \tilde{f}_-^{1*}(t_2) + \tilde{f}_+^0(t_1) \tilde{f}_+^{0*}(t_2) \right) t_2 \right) \\
& \left. \left. - \frac{|z_{-,f}^1(T)|^2 + |z_{+,f}^0(T)|^2}{2} (1 - 2\bar{n}\gamma T) \right\} \right]. \tag{B9}
\end{aligned}$$

Note that this expression still contains the endpositions of the zero temperature paths  $|z_{\pm,f}^j(T)|^2$ . Since these vanish if the compensation strategy is employed, this suggests that the strategy improves the fidelity even at finite temperatures. Furthermore, although all of the terms in the exponential are of first order of  $\gamma\bar{n}T$  we found that for our set of forces the dominating temperature dependent contribution would be the  $-4\bar{n}\gamma T$  terms. They arise because the finite temperature paths can no longer be closed reliably.

- 
- [1] R. P. Feynman, *International Journal of Theoretical Physics* **21**, 467 (1982).  
[2] M. Nielsen and I. L. Chuang, *Quantum Computation and Quantum Information* (Cambridge Univ. Press, 2000).  
[3] N. M. Linke, D. Maslov, M. Roetteler, S. Debnath, C. Figgatt, K. A. Landsman, K. Wright, and C. Monroe, *Proceedings of the National Academy of Sciences* **114**, 3305 (2017), <https://www.pnas.org/content/114/13/3305.full.pdf>.  
[4] T. P. Harty, D. T. C. Allcock, C. J. Ballance, L. Guidoni, H. A. Janacek, N. M. Linke, D. N. Stacey, and D. M.

- Lucas, *Phys. Rev. Lett.* **113**, 220501 (2014).  
[5] C. J. Ballance, T. P. Harty, N. M. Linke, M. A. Sepiol, and D. M. Lucas, *Phys. Rev. Lett.* **117**, 060504 (2016).  
[6] J. P. Gaebler, T. R. Tan, Y. Lin, Y. Wan, R. Bowler, A. C. Keith, S. Glancy, K. Coakley, E. Knill, D. Leibfried, and D. J. Wineland, *Phys. Rev. Lett.* **117**, 060505 (2016).  
[7] D. Wineland, C. Monroe, W. Itano, D. Leibfried, B. King, and D. Meekhof, *Journal of Research of the National Institute of Standards and Technology* **103**, 259 (1998).

- [8] D. S. Wang, A. G. Fowler, and L. C. L. Hollenberg, *Phys. Rev. A* **83**, 020302 (2011).
- [9] C. A. Sackett, D. Kielpinski, B. E. King, C. Langer, V. Meyer, C. J. Myatt, M. Rowe, Q. A. Turchette, W. M. Itano, D. J. Wineland, and C. Monroe, *Nature* **404**, 256 (2000).
- [10] D. Leibfried, B. DeMarco, V. Meyer, D. Lucas, M. Barrett, J. Britton, W. M. Itano, B. Jelenkovic, C. Langer, T. Rosenband, and D. Wineland, *Nature* **422**, 412 (2003).
- [11] A. Sørensen and K. Mølmer, *Phys. Rev. Lett.* **82**, 1971 (1999).
- [12] E. Solano, R. L. de Matos Filho, and N. Zagury, *Phys. Rev. A* **59**, R2539 (1999).
- [13] G. Milburn, S. Schneider, and D. James, *Fortschritte der Physik* **48**, 801 (2000).
- [14] M. Palmero, S. Martínez-Garaot, D. Leibfried, D. J. Wineland, and J. G. Muga, *Phys. Rev. A* **95**, 022328 (2017).
- [15] A. M. Steane, G. Imreh, J. P. Home, and D. Leibfried, *New Journal of Physics* **16**, 053049 (2014).
- [16] J. J. García-Ripoll, P. Zoller, and J. I. Cirac, *Phys. Rev. A* **71**, 062309 (2005).
- [17] J. J. García-Ripoll, P. Zoller, and J. I. Cirac, *Phys. Rev. Lett.* **91**, 157901 (2003).
- [18] V. M. Schäfer, C. J. Ballance, K. Thirumalai, L. J. Stephenson, T. G. Ballance, A. M. Steane, and D. M. Lucas, *Nature* **555**, 75 EP (2018).
- [19] M. Berry, *Proceedings of the Royal Society of London A: Mathematical, Physical and Engineering Sciences* **392**, 45 (1984), <http://rspa.royalsocietypublishing.org/content/392/1802/45.full.pdf>.
- [20] Y. Aharonov and J. Anandan, *Phys. Rev. Lett.* **58**, 1593 (1987).
- [21] G. Lindblad, *Communications in Mathematical Physics* **48**, 119 (1976).
- [22] V. Gorini, A. Kossakowski, and E. C. G. Sudarshan, *Journal of Mathematical Physics* **17**, 821 (1976), <https://aip.scitation.org/doi/pdf/10.1063/1.522979>.
- [23] D. M. Lucas, B. C. Keitch, J. P. Home, G. Imreh, M. J. McDonnell, D. N. Stacey, D. J. Szwer, and A. M. Steane, “A long-lived memory qubit on a low-decoherence quantum bus,” (2007), arXiv:0710.4421 [quant-ph].
- [24] T. Grotz, L. Heaney, and W. T. Strunz, *Phys. Rev. A* **74**, 022102 (2006).
- [25] W. T. Strunz, *Open Systems & Information Dynamics* **12**, 65 (2005).
- [26] W. Schleich, *Quantum Optics in Phase Space* (Wiley, 2011).
- [27] T. Feldker, H. Furst, H. Hirzler, N. V. Ewald, M. Mazzanti, D. Wiaters, M. Tomza, and R. Gerritsma, *Nature Physics* **16**, 413 (2020).
- [28] For the plot we used the results (B6) and (B8) instead of the final linearized expression (B9) since those provided better agreement in the rather strongly damped regime.
- [29] C. D. Bruzewicz, J. Chiaverini, R. McConnell, and J. M. Sage, *Applied Physics Reviews* **6**, 021314 (2019), <https://doi.org/10.1063/1.5088164>.